



Research Article

The potency of herbal extracts and its green synthesized nanoparticle formulation as antibacterial agents against *Streptococcus mutans* associated biofilms

Kulwadee Karnjana^a, Juntamanee Jewboonchu^a, Nattisa Niyomtham^d,
Paveen Tangngamsakul^c, Kingkan Bunluepuech^b, Lavnaya Goodla^e, Auemphon Mordmuang^{a,*}

^a Department of Medical Sciences, School of Medicine, Walailak University, Nakhon Si Thammarat, 80160, Thailand

^b Department of Applied Thai Traditional Medicine, School of Medicine, Walailak University, Nakhon Si Thammarat, 80160, Thailand

^c Walailak University Hospital, Walailak University, Nakhon Si Thammarat, 80160, Thailand

^d International College of Dentistry, Walailak University, Bangkok, 10400, Thailand

^e Department of Biochemistry and Molecular Biology, University of New Mexico School of Medicine, Albuquerque, NM, 87131, United States of America

ARTICLE INFO

Keywords:

Streblus asper

Cymbopogon citratus

Syzygium aromaticum

Green synthesized nanoparticle

Streptococcus mutans

ABSTRACT

This study aims to determine the effects of the extracts of *Streblus asper*, *Cymbopogon citratus*, *Syzygium aromaticum* and its formulation of green synthesized silver nanoparticle (AgNPs) on *Streptococcus mutans* growth and biofilm formation. The ethanolic extracts of *S. asper*, *C. citratus*, *S. aromaticum*, and a mix of the three herbs demonstrated antibacterial activity against *S. mutans* isolates by reducing bacterial biofilm formation and decreasing bacterial cell surface hydrophobicity. The formulated AgNPs from the ethanolic extracts could enhance the antibacterial activities of the plant extracts. Molecular docking found the best interaction between luteolin isolated from *C. citratus* and glucosyltransferase protein (GtfB), assuming the promising anti-biofilm activity. The scanning electron microscopy revealed morphological changes in the biofilm structure and a significant decrease in the biofilm area of the AgNPs treated. The study suggested that the extracts and its application could be used as natural alternative agents with multi-action against *S. mutans* infections.

1. Introduction

Prevalence of dental caries, oropharyngeal cancers, oral ulcers, and periodontal diseases are the most widespread oral common diseases worldwide [1]. The oral diseases affect up to 80% of the population in developing countries, both children and adults [2]. Oral health is interconnected with overall health and is related to a person's overall quality of life [3]. Dental caries is a biofilm-related oral disease driven by an interaction between the enamel surface and several factors, including microbial biofilm on the tooth surface, sugars, saliva, immunity, and genetics, in which dental hard tissues undergo phasic demineralization and remineralization [1,4]. Caries can occur at any stage of life, in both primary and permanent dentitions, and result in detrimental effects on the tooth crown and, in later years, on exposed root surfaces [1]. The demineralization and remineralization process on the tooth surface are related to the capacity of acid production by acidogenic bacteria that accumulate in dental plaque. *Streptococcus mutans* is the

main pathogenic acid-producing bacterium associated with dental plaque on tooth surfaces and is responsible for dental caries [5–7]. The formation of the complex structure of biofilms is a multistep process beginning with bacteria adhering to the implant's surfaces using cell wall-associated adhesins [8]. Bacterial exopolysaccharides are employed to promote second colonizer adherence, biofilm formation, and the protection of bacteria from the host immune response and antibiotic therapy [7,8]. Thus, limiting the population of *S. mutans* or decreasing biofilm formation are techniques for the prevention of caries [7,9].

Natural products derived from medicinal plants have proven to be an abundant source of biologically active compounds, and many of them have been the basis for the development of new lead chemicals for pharmaceuticals [10]. With respect to diseases caused by microorganisms, the increasing resistance of many common pathogens to currently used therapeutic agents, such as antibiotics and antiviral agents, has led to renewed interest in the discovery of novel anti-infective compounds.

* Corresponding author at: 222, School of Medicine, Walailak University, Nakhon Si Thammarat, 80160, Thailand.

E-mail address: auemphon.mo@wu.ac.th (A. Mordmuang).

<https://doi.org/10.1016/j.btre.2022.e00777>

Received 8 October 2022; Received in revised form 22 November 2022; Accepted 9 December 2022

Available online 11 December 2022

2215-017X/© 2022 The Authors. Published by Elsevier B.V. This is an open access article under the CC BY-NC-ND license (<http://creativecommons.org/licenses/by-nc-nd/4.0/>).

Streblus asper Lour (ST), *Cymbopogon citratus* (CY), and *Syzygium aromaticum* (SY) are the main herbal ingredients in Thai toothpaste formulations. *Streblus asper* Lour, commonly known as the “toothbrush tree”, presents various chemical constituents and phytochemical compounds, such as kamloside, asperoside, strebloside, indroside, cannodimemoside, strophalloside, strophanolloside, 16-O-acetylglucogitomethoside, glucogitodimethoside, glucokamloside, sarmethoside, and glucostrebloside [11]. This plant has also been used as a treatment for different ailments, such as filariasis, leprosy, toothache, diarrhea, dysentery, cancer, and diabetes [11,12]. *C. citratus*, lemongrass, is a potent natural bioproduct that is frequently utilized in food preservation due to its antibacterial and antioxidant properties [13]. The major phytochemical compounds are mainly terpenes, alcohols, ketones, aldehydes, and esters, including essential oils such as terpenes citral, neral, geraniol, nerol, citronellol, 1,8-cineole (eucalyptol), α -terpineol, linalool, and geranyl acetate [13,14]. Geraniol, neral, and eucalyptol, the essential oils of lemongrass, inhibit the production of bacterial biofilms formed by different foodborne pathogens, including *Bacillus cereus*, *B. subtilis*, *Escherichia coli*, *Klebsiella pneumoniae*, *Listeria monocytogenes*, *Pseudomonas aeruginosa*, *Salmonella choleraesuis*, and *Staphylococcus aureus* [13,15,16]. A clove of *S. aromaticum* is a source of several phytochemicals, including sesquiterpenes, monoterpenes, hydrocarbons, and phenolic compounds. The most abundant phytochemicals in clove oil are eugenol, eugenol acetate, and β -caryophyllene [17]. The plant and its compounds have been demonstrated to be effective against toothache, but biofilm and antibacterial activity studies are limited.

Furthermore, metal nanoparticles were formerly used in a variety of developmental activities, including agriculture, industry, medicine, and pharmaceuticals. Nanobiotechnology in combination with sustainable organic chemistry has enormous potential for producing innovative and critical components of structures that sustainably support the environment, human health, and industry [18]. Due to their diverse properties, nanoparticles (NPs) are a broad category of substances with diameters less than 100 nm that can be used in a variety of processes in a variety of sectors, including agriculture, materials and manufacturing, mechanical industries, medicine, pharmaceuticals, and the environment [19]. In particular, silver nanoparticles (AgNPs) have unique characteristics, such as the ease of converting Ag^{1+} to Ag^0 and chemical inertia, which make them the best choice for many applications, including antibacterial agents, biosensors, and chemical catalysts.

Moreover, the molecular docking technique, a computer-assisted technique, is useful for biological research with a potential approach for the prediction of molecular interactions between a natural product and a proteinaceous receptor. This technique is able to speculate the binding site at which a natural compound binds to the protein. Glucosyltransferases (Gtfs) engage the virulence factors in quorum sensing responsible for the cariogenic process of *S. mutans*-mediated dental caries. *S. mutans* possesses three types of Gtfs, including GtfB, which are essential for the assembly of *S. mutans* biofilms [20]. The aims of this study were to investigate the phytochemical profiles of *S. asper*, *C. citratus*, and *S. aromaticum*, formulate green AgNPs synthesized from herbal plant extracts and determine their antibacterial activities against *S. mutans* and antibiofilm formation.

2. Materials and methods

2.1. Materials

Acetonitrile and methanol (HPLC grade) were purchased from RCI Labscan (Bangkok, Thailand). Deionized water (18.2 M Ω -cm) was purified using a Milli-Q system (Millipore, Billerica, MA, USA). Ethanol and formic acid (analytical grade) were purchased from Merck (Darmstadt, Germany).

2.2. Plant materials and preparation of herbal extracts

Dry *Cymbopogon citratus* (leaf and stem), *Streblus asper* (bark), and *Syzygium aromaticum* (flower) were collected in 2021 from the Phrom Khiri District, Nakhon Si Thammarat Province, Thailand. Herbarium voucher specimens were *Cymbopogon citratus* SM 0,324,030,901, *Streblus asper* SM1920011903, and *Syzygium aromaticum* SM1925011802. They were deposited at Applied Thai Traditional Medicine, School of Medicine, Walailak University, Nakhon Si Thammarat, Thailand. The plant materials were dried using a hot air oven at 60 °C for 72 h. All dried herbs were ground to coarse powders. To obtain crude ethanolic extracts, pulverized herbs were macerated in 95% ethanol (1:10 w/v) for 7 days. For aqueous extracts, the herbs were subjected to 6-hour cycles of Soxhlet extraction. The macerates were then filtered and dried using a rotary evaporator. The crude extracts were stored at -20 °C until further use. To obtain the mixed herb formulation, the three plant extracts were mixed at 1:1:1 w/w. The plant extracts were dissolved in dimethyl sulfoxide (DMSO) and dilute to obtain a final concentration of the solvent less than 10% before use for antibacterial testing.

2.3. Qualitative phytochemical analysis of herbal extracts

To identify the compounds in herbal extracts, high-performance liquid chromatography coupled to high-resolution mass spectrometry (HPLC-MS) was used. Herbal extract was prepared at 2.5 mg/ml in methanol and filtered through a 0.45 μm membrane filter. The HPLC system (UltiMate® 3000 system, Thermo Fisher Scientific, Dionex Softron GmbH, Dornierstr. 4, Germany) was utilized with a reverse-phase column (C18 analysis column, 2.1 mm x 150 mm and 3 μm particle size, Thermo Fisher Scientific, Sunnyvale, CA). The separation was performed by a gradient elution program of 0.1% formic acid in water (component A) and acetonitrile (component B) at a flow rate of 0.3 ml/min. The gradient system for HPLC was as follows: 0–30 min, 5–55% B; 30–40 min, 55–95% B; and 40.1–45 min, 5% B. The injection volume was 2 μl , and the column temperature was 40 °C. The isolated components from the HPLC system were subjected to high-resolution mass spectrometry (micrOTOF-Q-II, Bruker Daltonik, Bremen, Germany). The negative ion and positive ion modes of electrospray ionization (ESI) systems were used to generate mass to charge ratio (m/z) values in a range of 50–1000. The mass spectrometric conditions were optimized as follows: dry temperature, 200 °C; drying gas flow rate, 8.0 l/min; and nebulizer gas pressure, 2.0 bar. The capillary voltage was set at 3 kV and 4.5 kV in the negative and positive ion modes, respectively. Isolated compounds were examined by comparing the calculated mass values from previously available data with the obtained m/z values. Differences found that were less than 30 parts per million (ppm) were considered acceptable.

2.4. Synthesis of silver nanoparticles from herbal ethanolic extracts

The green synthesis of silver nanoparticles (AgNPs) was performed as previously described [21]. Briefly, an aqueous solution of 1 mM silver nitrate (AgNO_3) was reacted with 0.01% (w/v) ethanolic plant extract at a final concentration for synthesis. The mixture was kept in the dark at 28 °C at 150 rpm for 48 h in a rotary shaker operating at 150 rpm for 48 h. The bioreduction of Ag^+ ions in the reaction medium were measured by UV-visible spectrophotometry (Perkins Elmer LAMBDA 25 UV/Vis spectrophotometer, Waltham, MA, USA) at wavelengths of 200–800 nm. The mixture without AgNO_3 and the ethanolic extract itself were used as controls in the synthesis. Silver nanoparticle solutions were purified by centrifugation at 14,500 rpm for 1 h, and the pellet was resuspended in sterile distilled water. Nonreduced AgNO_3 ions and unbound extract residues were removed by repeated centrifugation steps 3 times, as described above. The amount of the extract was estimated by spectrophotometry using its absorbance at 670 nm. The collected pellet was resuspended in sterile distilled water and checked for sterility before

use.

2.5. Bacterial isolates and culture conditions

Twenty-six isolates of *S. mutans* clinical strains were obtained from a dental clinic at Nopphitam Hospital in Nakhon Si Thammarat, Thailand. The isolates were identified by bacterial growth on Mitis-sucrose-bacitracin (MSB) agar (Difco, USA) and confirmatory tests with biochemical test kits (RapidITM Systems, Thermo Fisher Scientific, USA). The bacterial isolates were cultured in sterile brain heart infusion (BHI) broth and incubated at 37 °C in the presence of 5% CO₂. After 48 h of incubation, Gram staining was performed, and the cultures were replated to verify bacterial isolation. The bacteria were transferred to broth media for antibacterial activity testing. The bacterial suspensions were adjusted to a concentration equal to the No. 0.5 McFarland standards (1.5×10^8 CFU/mL) (DEN-1 Densitometer; suspension turbidity detector, BIOSAN, Latvia) and further diluted in normal saline solution (NSS) to obtain a bacterial concentration of 1×10^6 CFU/mL. The identified isolates were named clinical *Streptococcus mutans* (CSM01-CSM26). *S. mutans* ATCC 25,175 was obtained from the American-type culture collection for use as a reference strain in this study.

2.6. Growth of bacterial biofilm and biofilm inhibition assay

S. mutans ATCC 25,175 was cultured overnight in BHI media. The culture was adjusted to the turbidity of a 0.5 McFarland standard or a measured optical density (OD) of 1.0 (approximately 1×10^8 CFU/mL) at 600 nm. The bacterial suspensions were diluted 1:100 in 1 mL of BHI broth containing 2% sucrose (Merck, Darmstadt, Germany) and were then transferred into sterile round-bottom 96-well polystyrene microplates (SPL Life Sciences Co., Korea). The bacterial biofilm was grown at 37 °C for 24 h. To evaluate the effects of the herbal extracts on bacterial biofilm formation, the different concentrations at the subminimum inhibitory concentration and minimum inhibitory concentration of each extract were subjected to the bacterial culture and grown at 37 °C for 24 h. After incubation, the culture wells were gently washed twice with sterile phosphate buffered saline (PBS, pH 7.3) and air-dried. An aliquot of 200 µL of 0.1% crystal violet solution (Merck, Darmstadt, Germany) was added to each well to stain the bacterial biofilm for 15 min at room temperature. Any excess stain was removed by rinsing with distilled water and allowed to dry. The biofilm biomass on the CLs was determined by decolorization with 200 µL of 33% acetic acid for 15 min and quantified by measuring the OD at 570 nm using a microtiter plate reader (BioTek Instruments, Inc., USA). All experiments were performed in triplicate and repeated three times.

2.7. Screening for antimicrobial activity by the agar disk diffusion assay

The antimicrobial activity of the aqueous and ethanolic extracts was determined by the agar disk diffusion method. Broth culture of the bacterial strain was adjusted to the density of 0.5 McFarland standard. An aliquot of 0.1 mL of the bacterial suspension was spread on BHI agar plates. The 6-mm diameter paper discs loaded with 15 mg of extract were placed on the media and incubated at 37 °C overnight. Zones of growth inhibition were measured in millimeters. A standard disk of 0.2% chlorhexidine was used as a positive control, while a disk of 10% DMSO was used as a negative control. All tests were performed in triplicate, and the mean values of the diameter of the inhibition zone \pm standard deviation were determined [22].

2.8. Determination of the minimum inhibitory concentration (MIC) and minimum bactericidal concentration (MBC)

The antibacterial activities of both aqueous and ethanolic extracts, including synthesized AgNPs from the plant ethanolic extracts (NPs) were measured by the broth microdilution method according to the

Clinical and Laboratory Standards Institute (CLSI) guidelines (2018). In a 96-well microtiter plate, 20 µL aliquots of the agents were separately added and diluted by two-fold serial dilution from their original concentrations. The total volume was made up to 100 µL by adding 80 µL of Mueller-Hinton broth into each well. One hundred microliters of bacterial suspension (10^6 CFU/mL) was inoculated in the broth containing the extract and incubated at 37 °C for 18 h. MHB media was included as a negative control. The minimum bactericidal concentration (MBC) was subsequently determined by taking aliquots of the MIC wells and striking on BHI agar plate. An aliquot of 100 µL from each well with an MIC value was plated on tryptic soy agar (TSA) and incubated at 37 °C for 18–24 h. The plates were observed for the appearance of bacterial growth, and the MBC value was determined. The experiment was carried out in triplicate.

2.9. Microbial adhesion to hydrocarbon (MATH) test

The cell-surface hydrophobicity of *S. mutans* was measured by the MATH test [21]. The bacterial isolates were maintained in BHI medium supplemented with the final concentration of 1/4 to 2 \times the MIC of the plant ethanolic extract at 37 °C for 3–5 h. After incubation, the bacterial cells were collected by centrifugation at 4000 \times g for 5 min and washed twice with sterile saline solution. The cell density was adjusted to an OD of 0.3 at 600 nm (OD initial). Bacterial cells incubated without the extract were used as a control. Three milliliters of the cell suspension were placed in a glass tube, and 0.25 mL of toluene was added. The mixtures were thoroughly mixed for 2 min by vortexing and allowed to equilibrate at room temperature for 10 min. After the toluene phase had separated from the culture phase, the OD of the aqueous phase (OD final) was determined at 600 nm by spectrophotometry. The hydrophobicity index (%) was calculated as follows: [(O.D. initial - O.D. final)/O.D. initial] \times 100. The isolate of *S. mutans* with a hydrophobic index greater than 60% was classified as hydrophobic.

2.10. Molecular docking study

The molecular interactions between the bioactive compounds of plants and quorum sensing protein, which is related to biofilm formation, determined the scoring and binding interactions in a protein binding pocket using computation methods. The 3D structures of the natural compounds, chlorhexidine as a commercial drug, and glucosyl-transferase protein (GtfB) (PDB code: 3AIB) from *S. mutans* were obtained from public databases. Before beginning docking, the binding site of the receptor was specified. The molecular docking technique was performed by the AutoDock 4.2 package to examine the binding modes of natural compounds and the protein compared to commercial drugs. The natural compounds and protein were in PDBQT files and generated a protein receptor grid size of 126 Å \times 126 Å \times 126 Å in x, y, and z, respectively, with a grid spacing of 0.375 in the specific area of inhibitor binding. The number of runs for each docking was set to 50 with a population size of 200 using the Lamarckian genetic algorithm implemented by the AutoDock 4.2 package. The calculation of the binding score was previously described [23]. Candidate poses were minimized in the context of the active site using a grid-based method for evaluating protein ligand interaction energies.

2.11. Morphological observation of *S. mutans* biofilms by scanning electron microscopy (SEM)

S. mutans ATCC 25,175 biofilms were prepared by a previously described method with slight modification [24]. Briefly, biofilms were formed on 5-mm diameter round coverslips in a flat-bottom 24-well polystyrene plate. Each NP compound and 0.2% chlorhexidine standard solution were added to the wells at the MIC. To grow the mono-species biofilm, a culture medium with 2% sucrose (1 mL) containing *S. mutans* cells (10^8 CFU/mL) was anaerobically incubated at

37 °C. After 24 h of biofilm formation, the coverslips were transferred to wells containing 1 mL of 2.5% glutaraldehyde solution overnight. Then, the fixed specimens were gently washed twice with phosphate-buffered saline (PBS). The sample was exposed to 1% osmium tetroxide (OsO₄) for 1 h and then dehydrated with an ethanol concentration series (50%, 70%, 85%, 90%, 95%, and 2 × 100%) for 15 min in each solution. The biofilm samples were dried in a desiccator and then coated with gold in a Cressington 108 Auto Sputter Coater (Cressington Scientific Instruments, UK). Each coverslip was subjected to electron microscopy (Merlin Compact, Zeiss, Germany) at The Center for Scientific and Technological Equipment (CSE), Walailak University. The surface topographies of biofilm specimens were examined using the secondary electron emission mode with an accelerating voltage of 5 kV. The magnifications used were × 1000, × 10,000, and × 30,000. The bacterial biofilm formation on each surface was quantified using ImageJ program analysis by calculating the percentage of the area on the coverslips. Each image's histogram was calculated to determine the number of red pixels representing the biofilm area. The percentage of biofilm remaining on the surface was calculated as follows: Percentage of biofilm remaining = [Biofilm area/Total surface area] × 100.

2.12. Statistical analysis

Values of each parameter are expressed as the mean ± standard error of the mean (SEM). Comparisons among different groups were performed by one-way analysis of variance (ANOVA). When significant differences existed, Dunnett's multiple range tests were used to compare the means. A probability of $p < 0.05$ was considered significant.

3. Results

3.1. Preliminary antibacterial activities of the herbal extract fractions against *S. mutans*

The antibacterial activity of the plant extracts was preliminarily tested by agar disk diffusion. The results are shown in Table 1. The bacterial inhibitory activity of the ethanolic plant extracts was considerably greater than the activity of the extracts from the aqueous fractions. The inhibition zone of the ethanolic extract of each herbal plant against *S. mutans* ATCC 25,175 ranged from 7.9–16.2 mm. The aqueous extracts showed inhibitory activity against *S. mutans* ATCC 25,175 ranging from 6.5–14.6 mm. The ethanolic extract of *S. aromaticum* demonstrated the largest inhibition zone against 26 clinical isolates, ranging from 16.1 to 18.3 mm. The ethanolic extracts of *S. asper* and *C. citratus* produced inhibition zones against the clinical isolates ranging from 8.1 to 9.3 mm and 7.1 to 8.2 mm, respectively. Moreover, the mixed herb extract exhibited greater inhibitory activity than the crude extracts from single plants. The inhibition zones of the aqueous fraction and the ethanolic fraction from the mixed herbs against *S. mutans* ATCC 25,175 were 14.6 mm and 15.9 mm, respectively. The ethanolic extract

Table 1

. Inhibition zone of the herbal extracts against *S. mutans* clinical isolates on agar culture.

Testing agents	Fractions	Diameter of inhibition zone (mm)	
		<i>S. mutans</i> ATCC 25,175	Clinical isolates (N = 26)
<i>S. asper</i>	Aqueous	7.3 ± 0.22	6.5 ± 0.32–7.8 ± 0.11
	Ethanolic	8.6 ± 0.31	8.1 ± 0.23–9.3 ± 0.12
<i>S. aromaticum</i>	Aqueous	14.4 ± 0.15	12.5 ± 0.13–14.2 ± 0.06
	Ethanolic	16.2 ± 0.51	16.1 ± 0.06–18.3 ± 0.12
<i>C. citratus</i>	Aqueous	6.5 ± 0.21	6.9 ± 0.01–7.9 ± 0.15
	Ethanolic	7.9 ± 0.27	7.1 ± 0.13–8.2 ± 0.12
Mixed herbs	Aqueous	14.6 ± 0.21	7.8 ± 0.22–8.9 ± 0.16
	Ethanolic	15.9 ± 0.34	18.1 ± 0.32–20.3 ± 0.11
0.2% Chlorhexidine	–	21.5 ± 0.12	19.8 ± 0.25–23.3 ± 0.12

of mixed herbs demonstrated better antibacterial activity against the 26 clinical isolates than its aqueous extract, which provided clear zones in a range of 18.1 to 20.3 mm, which is close to the activity of the standard of 0.2% chlorhexidine.

3.2. MIC and MBC of the plant extracts and their green AgNPs synthesized against *S. mutans*

The MIC and MBC values of the herbal extracts and their synthesized NPs are shown in Table 2. The MIC and MBC of the ethanolic extracts of each plant, including the mixed herbs, were significantly higher than those of the aqueous extracts. The ethanolic extracts showed antibacterial activity against *S. mutans* ATCC 25,175 with MICs and MBCs ranging from 0.512 to 2.084 mg/mL and 1.024 to 4.096 mg/mL, respectively, while the aqueous extracts demonstrated MICs and MBCs ranging from 2.048 to 4.096 mg/mL and 4.096 to 16.384 mg/mL, respectively. The activity of the extracts to inhibit *S. mutans* clinical strains was evaluated in terms of the MIC₉₀ and MBC₉₀ values. The ethanolic extracts of *S. aromaticum*, *S. asper*, *C. citratus*, and mixed herbs possessed MIC₉₀/MBC₉₀ values of 1.024/2.048, 2.048/4.096, 2.048/8.192, and 0.512/2.048 mg/mL, respectively. Furthermore, the inhibitory activity of AgNPs formulated from the herbal extracts against *S. mutans* was determined. The results showed that the application of AgNPs could decrease the inhibitory concentration of the ethanolic extracts by a 4- to 8-fold reduction. Remarkable antibacterial activity was observed in the formulations of AgNPs from the mixed herb extract, with MICs/MBCs and MIC₉₀/MBC₉₀ values of 0.064/0.128 and 0.064/2.048 mg/mL, respectively.

3.3. Phytochemical components of herbal extracts

The ethanolic extracts of *S. asper*, *S. aromaticum*, and *C. citratus* and the ethanolic extract of mixed herbs exhibited higher antibacterial activity than the aqueous extracts. Thus, the qualitative analysis of the ethanolic extracts was performed using the HPLC–MS technique. Both negative and positive ionization modes were used to identify the chemical compositions of individual herbs as well as the mixed herbs. Based on previous studies, we were able to predict candidate compounds in each extract responsible for the antibacterial activities. The proposed negative and positive ions of compounds that showed the antibacterial properties of each extract are revealed in Table 3. Vanillin (1), 3,3'-methylene-bis(4-hydroxybenzaldehyde) (2), and palmitic acid (3) were found in *S. asper*. Seven compounds, gallic acid (4), biflorin (5), quercetin (6), kaempferol (7), eugenol (8), rhamnocitrin (9), 2,3,4-trimethoxyacetophenone (10), and copaene (11), were identified from *S. aromaticum*. Five metabolites were found in *C. citratus*, including

Table 2

MIC and MBC of herbal extracts and their green-synthesized AgNP formulations against *S. mutans* ATCC 25,175 and clinical isolates.

Testing agents	Fractions	MIC/MBC (mg/mL)	MIC ₉₀ /MBC ₉₀ (mg/mL)
		<i>S. mutans</i> ATCC 25,175	Clinical isolates (N = 26)
<i>S. asper</i>	Aqueous	4.096/8.192	4.096/16.384
	Ethanolic	2.048/2.048	2.048/4.096
	NPs	0.265/0.512	0.128/0.512
<i>S. aromaticum</i>	Aqueous	2.048/4.096	4.096/8.192
	Ethanolic	0.512/1.024	1.024/2.048
	NPs	0.064/0.265	0.128/2.048
<i>C. citratus</i>	Aqueous	4.096/16.384	4.096/16.384
	Ethanolic	2.048/4.096	2.048/8.192
	NPs	0.512/1.024	0.512/2.048
Mixed herbs	Aqueous	2.048/4.096	4.096/8.192
	Ethanolic	0.512/1.024	0.512/2.048
	NPs	0.064/0.128	0.064/2.048
0.2% Chlorhexidine	–	0.0093/0.018	0.018/0.036

Table 3
Proposed chemical components in medicinal herbal extracts.

Extraction	Compound	TR (min)	Positive ion (m/z)		Negative ion (m/z)		Molecular formula	Error (ppm)	Proposed compounds	Reference
			Measured	Calculated	Measured	Calculated				
<i>S. asper</i>	1	7.789			151.0408	151.0401	C ₇ H ₆ O ₂	1.4	Vanillin	[1]
	2	11.675			257.0459	257.0455	C ₁₄ H ₁₀ O ₅	0.2	3,3'-Methylene-bis(4-hydroxybenzaldehyde)	[2]
<i>S. aromaticum</i>	3	33.929	257.2472	257.2475			C ₁₆ H ₃₄ O ₂	1.0	Palmitic acid	[1,3]
	4	3.072			169.0138	169.0142	C ₇ H ₆ O ₅	-2.5	Gallic acid	[4]
	5	6.672	355.1016	355.1023	353.0882	353.0878	C ₁₆ H ₁₉ O ₉	1.3	Biflorin	[4]
	6	9.679	303.0485	303.0499			C ₁₅ H ₁₀ O ₇	4.5	Quercetin	[5]
	7	12.969	287.0546	287.0550			C ₁₅ H ₁₀ O ₆	-1.4	Kaempferol	[6]
	8	17.523	165.1793	165.1794			C ₁₀ H ₁₂ O ₂	1.9	Eugenol	[7]
	9	18.465	301.0700	301.0706			C ₁₆ H ₁₃ O ₆	1.9	Rhamnocitrin	[6]
	10	19.628	211.0964	211.09649			C ₁₁ H ₁₄ O ₄	0.3	2,3,4-Tri-methoxyacetophenone	[8]
	11	29.775	203.1795	203.1794			C ₁₅ H ₂₂	-0.6	Copaene	[8]
	<i>C. citratus</i>	7	12.962	287.0545	287.0550	285.0568	285.0557	C ₁₅ H ₁₀ O ₆	1.2	Kaempferol
12		13.880	221.1899	221.1897			C ₁₅ H ₂₄ O	0.0	β -Caryophyllene oxide	[11]
13		14.664	287.0549	287.0550			C ₁₅ H ₁₀ O ₆	0.4	Luteolin	[9,10]
14		16.362	203.1794	203.1794			C ₁₅ H ₂₂	-0.1	β -Vatirenene	[11]
15		23.354	205.1957	205.1950			C ₁₅ H ₂₄	3.4	Isocaryophyllene	[11]
Mixed Herbs	4	2.603			169.0133	169.0142	C ₇ H ₆ O ₅	0.4	Gallic acid	[4]
	16	6.570	355.1019	355.1023	353.0872	353.0878	C ₁₆ H ₁₈ O ₉	1.0	Chlorogenic acid	[4]
	6	9.711	303.0487	303.0499			C ₁₅ H ₁₀ O ₇	4.0	Quercetin	[5]
	13	10.495	287.0538	287.0550			C ₁₅ H ₁₀ O ₆	-4.0	Luteolin	[9,10]
	17	10.712	317.0647	317.0655			C ₁₆ H ₁₂ O ₇	2.6	Rhamnetin	[6]
	18	12.138			447.1282	447.1296	C ₂₂ H ₂₄ O ₁₀	1.4	Quercetin 3'-O-glucuronide	[6]
	7	12.954	287.0541	287.0550	285.0396	285.0404	C ₁₅ H ₁₀ O ₆	0.8	Kaempferol	[6]
	19	24.356	203.1794	203.1794			C ₁₅ H ₂₂	-1.6	β -Vatirenene	[11]
	20	24.356			562.3285	563.3225	C ₃₁ H ₄₈ O ₉	2.6	5- β H-16 β -hydroxylkamaloside	[2]
	3	33.922	257.2469	257.2475			C ₁₆ H ₃₂ O ₂	-2.0	Palmitic acid	[3]

kaempferol (7), β -caryophyllene oxide (12), luteolin (13), β -vatirenene (14), and isocaryophyllene (15). The compounds that were found in each of the ethanolic extracts were also found in the toothpaste formulated. These included gallic acid (4), chlorogenic acid (16), quercetin (6), luteolin (13), rhamnetin (17), quercetin 3'-O-glucuronide (18), kaempferol (7), β -vatirenene (19), 5- β H-16 β -hydroxylkamaloside (20), and palmitic acid (3).

3.4. Inhibitory activity of *S. mutans* biofilm formation

The effects of the herbal ethanolic extracts on reducing *S. mutans* ATCC 25,175 biofilm production are shown in Fig. 1. The bacterial cells were treated with different concentrations of each extract at $1/4 \times$ MIC,

$1/2 \times$ MIC, and the MIC for 24 h before the determination of biofilm formation. The percentage of bacterial biofilm reduction was evaluated by comparing the biofilm density in the treatments with that in the nontreated culture. The results showed that the inhibitory activity of all extracts occurred in a concentration-dependent manner. The percentages of biofilm inhibition of the ethanolic extracts of *S. asper*, *S. aromaticum*, *C. citratus* and mixed herbs at a concentration of $1/4 \times$ MIC were 58.00%, 57.67%, 58.33%, and 59.67%, respectively, which were similar to the inhibitory effects of those extracts at $1/2 \times$ MIC, with no significant difference (p value > 0.05). The ethanolic extracts of *S. asper*, *S. aromaticum*, *C. citratus*, and mixed herbs at the MIC demonstrated inhibitory effects by reducing the bacterial biofilm to 77.67%, 66.67%, 71.33%, and 76.00%, respectively.

3.5. Effects of herbal extracts on *S. mutans* cell surface hydrophobicity

The effects of the plant ethanolic extracts on the surface properties of the bacterial cell were determined, as it had been hypothesized that the extract may modify the hydrophobicity or aggregation activity of the bacteria (Fig. 2). The *S. mutans* ATCC 25,175 strain and two clinical isolates, CSM06 and CMS25, were classified as hydrophobic bacteria with a hydrophobicity index greater than 60% in this study. Furthermore, the bacterial cells treated with the ethanolic extracts of *S. asper*, *S. aromaticum*, *C. citratus*, and mixed herbs exhibited a lower level of hydrophobicity than the untreated cells. The ethanolic extract modified the bacterial cell surface by decreasing the hydrophobicity in a concentration-dependent manner. The concentration of $1/4 \times$ MIC of all tested extracts could significantly reduce the cell hydrophobicity of *S. mutans* ATCC 25,175 (Fig. 2A) and both CSM06 and CSM25 isolates (Fig. 2B-C). The hydrophobicity indices of the bacterial isolates were significantly decreased to reach an index lower than 50% by exposure to $1/2 \times$ MIC ethanolic extracts.

3.6. Molecular docking analysis

The molecular interaction between the bioactive compounds and protein target was determined by the molecular docking technique. The

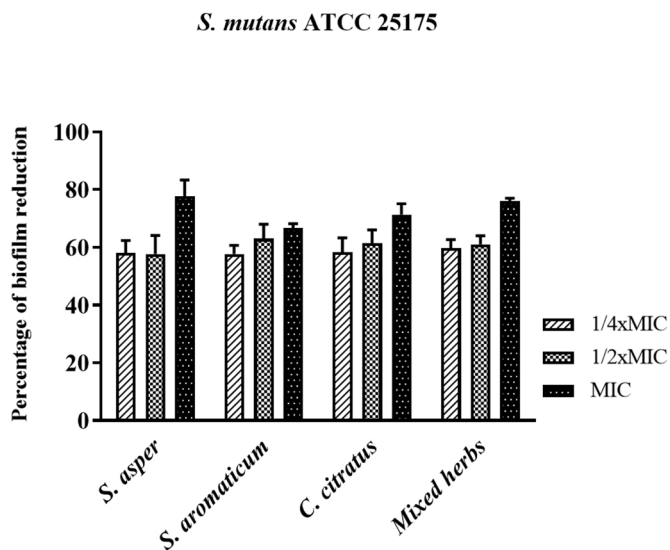


Fig. 1. Demonstration of *S. mutans* biofilm reduction by treatment with the herbal extracts at concentrations of $1/4 \times$ MIC, $1/2 \times$ MIC, and $1 \times$ MIC.

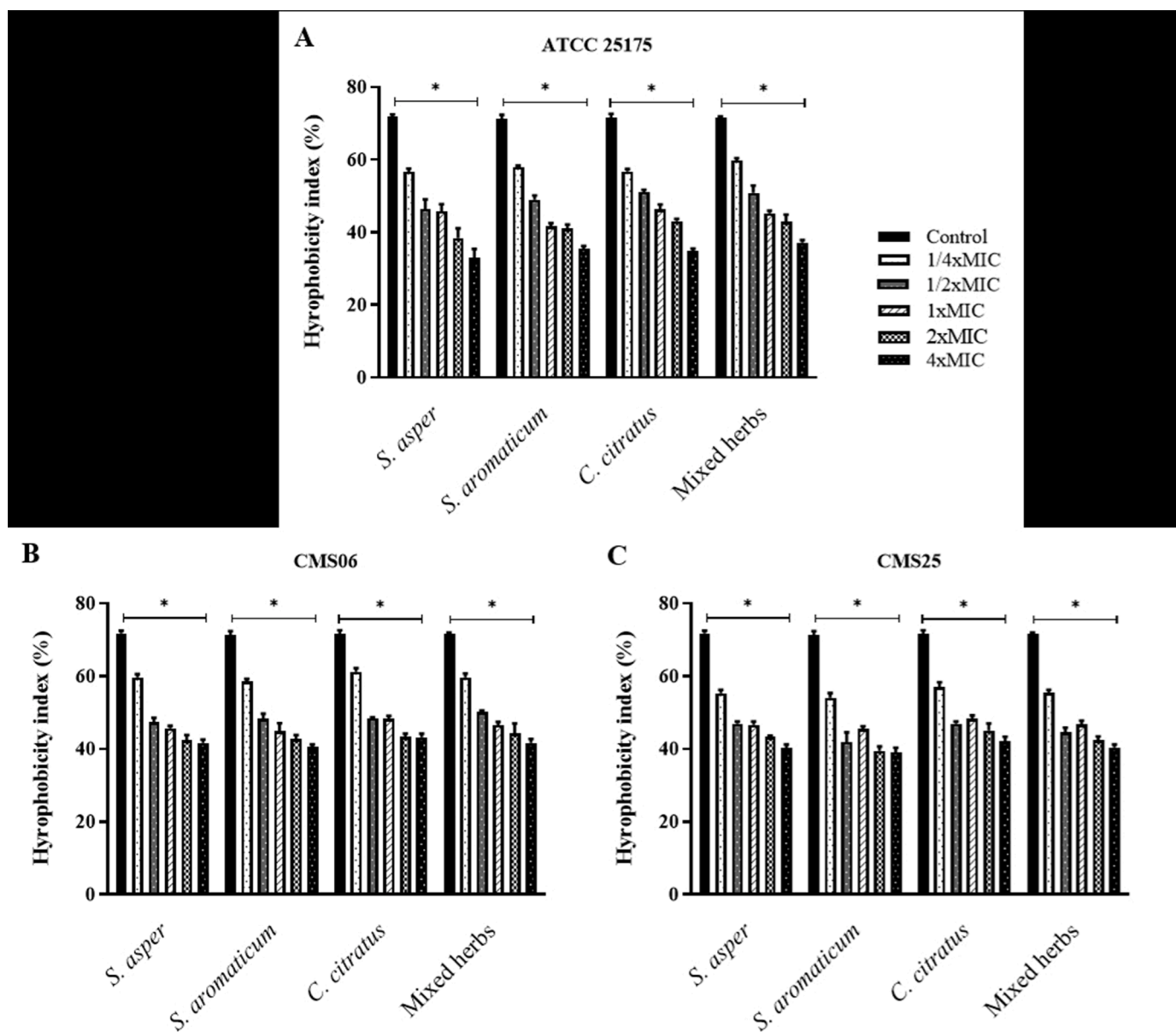


Fig. 2. . Effects of the ethanolic extracts of *S. asper*, *S. aromaticum*, *C. citratus*, and mixed herbs on the cell surface hydrophobicity of *S. mutans* ATCC 25,175 (A), CSM06 (B), and CMS25 (C). The hydrophobicity index was quantified by an assay for microbial adhesion to hydrocarbons (MATH) after treating the bacterial cells with $1/4 \times \text{MIC}$, $1/2 \times \text{MIC}$, $1 \times \text{MIC}$, $2 \times \text{MIC}$, and $4 \times \text{MIC}$ of the extract. The natural hydrophobicity of the bacterial cells was observed in a control/nontreatment. The mean value \pm SD from at least duplicates is illustrated. * $p < 0.05$ demonstrated a significant difference between the tests and the control.

results are summarized in Table 4. A range of binding energies was observed, with several compounds comparable to the commercial drug. The lowest ΔG_{bind} and K_i describe the most favorable ligand conformation bound to the protein target and imply higher binding affinity. The result demonstrated that the binding score of the luteolin compound of *C. citratus* showed a high docking score, assuming an *in vitro* biofilm inhibitor.

The best-docked compound structure, visualized by the visual molecular dynamics (VMD) program, showed interacting molecules (Fig. 3). Nine amino acids were within a distance not exceeding 3 Å (hydrophobic interaction (yellow), Gly693; hydrogen bonds (red), Ala573, Glu574, Asn650, and Val691; charge interaction (blue), Lys651, Arg687, Arg712, and Asp852).

3.7. Micromorphology of *S. mutans* biofilms treated with AgNP formulations

The biofilms of *S. mutans* were treated with the green synthesized AgNP formulations from the herbal ethanolic extracts at the MIC. The SEM images showed AgNP sizes in the range of 53.38 ± 9.56 to 71.86 ± 2.82 nm. The biofilm morphological changes were observed by SEM. The *S. mutans* biofilms were composed of aggregated cocci in the chain with fibril filaments and structures resembling extracellular matrix. After the 24-hour biofilm formation, the control SEM image revealed all stages of bacterial formation, including the initial stage of bacteria attaching to the base material, the development of microcolonies, and the mature biofilm completely covered in an extracellular polysaccharide matrix. The final stage was observed as depressions in the matrix, which correspond to the vacated matrix spaces left by dispersed bacteria (Fig. 4). The effects of the synthesized AgNP formulations and

Table 4
Candidates of the bioactive compounds and GtfB protein using molecular docking.

Compounds	Binding energy (ΔG) Kcal/mol	Inhibitory constant (K_i) μM
Chlorhexidine (commercial drug)	-16.04	1.75×10^{-6}
<i>C. citratus</i>		
Luteolin	-9.39	0.13
Kaempferol	-9.22	0.17
Isocaryophyllene	-8.89	0.31
β -Caryophyllene oxide	-8.33	0.79
β -Vatirenene	-8.22	0.95
<i>S. asper</i>		
3,3-Methylenbis(4-hydroxybenzaldehyde)	-7.59	2.71
Vanillin	-5.72	64.17
Palmitic acid	-4.85	278.05
<i>S. aromaticum</i>		
Quercetin	-9.27	0.16
Kaempferol	-9.22	0.17
Rhamnocitrin	-8.73	0.40
Copaene	-8.56	0.54
Biflorin	-8.30	0.83
Gallic acid	-7.59	2.71
2,3,4-Tri-methoxyacetophenone	-6.90	8.73
Eugenol	-6.50	17.34
Mixed Herbs		
Luteolin	-9.39	0.13
Quercetin	-9.27	0.16
Kaempferol	-9.22	0.17
Rhamnetin	-8.97	0.27
β -Vatirenene	-8.22	0.95
Gallic acid	-7.59	2.71
Chlorogenic acid	-6.77	10.94
Quercetin 3'-O-glucuronide	-6.42	19.52
Palmitic acid	-4.85	278.05
5- β -H-16 β -hydroxylkamaloside	-	-

standard 0.2% chlorhexidine on the bacterial biofilm were assessed by image visualization and are shown in Fig. 5. The image of the untreated control revealed a dense pack of bacterial cells almost completely covered by the extracellular polysaccharide matrix and a small number of base materials, as shown in Fig. 5A. The reduction of bacterial biofilms on the base material was observed in the treatments of all tested AgNP formulations from the plant extracts. The images of 0.2% chlorhexidine and AgNPs from *C. citratus* treatments showed the clearest biofilm accumulation with a significant reduction in cell number. The bacterial cells were arranged in a chain structure without the extracellular matrix, as illustrated in Fig. 5B and D, respectively. Damaged cells with multiple pores were observed in the group treated with 0.2% chlorhexidine (Fig. 5B), whereas smooth cell membranes were observed in the group treated with AgNPs from *C. citratus*. Some fibroform extracellular matrix-like structures with partially maintained extracellular matrix were observed on the surface of biofilms that were treated with the AgNP formulations from mixed herbs (Fig. 5C), *S. aromaticum* (Fig. 5E), and *S. asper* (Fig. 5F).

Furthermore, the images taken at a magnification of $\times 1000$ were used to analyze the area of bacterial cell attachment on the surface using ImageJ software. The percentage of the remaining biofilm area was evaluated by calculating the number of pixels corresponding to the total bacteria in the image (Fig. 6A). The results demonstrated that the untreated control comprised $80.4 \pm 3.0\%$ of the surface area. The treatments of 2% chlorhexidine and AgNPs from *C. citratus* resulted in dramatic decreases in the area to 8.6 ± 1.5 and $8.9 \pm 1.8\%$, respectively. The AgNPs from mixed herbs, AgNPs from *S. aromaticum*, and AgNPs from *S. asper* decreased the biofilm area by 32.0 ± 1.6 , 38.8 ± 2.8 , and $45.4 \pm 3.3\%$, respectively (Fig. 6B).

4. Discussion

Dental caries is a costly biofilm-associated infectious disease caused by *S. mutans* that affects most of the world's population. The bacterium has been established as a major cariogenic bacterium causing dental caries in 60–80% of children and 100% of the adult population [25]. The cariogenic exopolysaccharide (EPS) mainly contributed by biofilm producing *Streptococcus* strain including some *S. mutans*, and it has been considered a virulence determinant for bacterial survival and pathogenicity in the host oral cavity. The acid production of the bacteria in the presence of fermentable carbohydrates leads to bacterial dysbiosis [26]. The mechanism facilitated bacterial colonization and biofilm adherence to the enamel surface, which caused plaque accumulation and tooth structural damage [27]. Thus, targeting the mechanism of EPS could be useful in preventing cariogenic biofilm formation. Inhibiting EPS production, suppressing EPS-related gene expression and regulatory mechanisms and destroying the matrix structure could be effective strategies for preventing infectious diseases [7]. Since tooth decay and tooth loss are associated with the consequences of plaque formation, many effective methods have been introduced to reduce oral plaque. Antibiotics and chemical agents are generally used in the field of dentistry for aseptic surgery and treatment. *S. mutans* has also been reported to have developed multidrug resistance [28,29]. As a result of rising drug-resistant bacteria, infectious diseases remain a significant concern in dental medicine. This fact will encourage the development of novel potential interventions for bacterial infectious diseases, including multidrug resistance and biofilm formation.

The use of alternative substances from natural compounds and nanoparticle technologies has been considered. There are some reports of *Lactococcus* producing bacteriocin nisin against relevant oral pathogenic bacteria. The study showed that nisin A could inhibit the growth of cariogenic streptococci, including *Streptococcus gordonii*, *Streptococcus sanguinis*, *Streptococcus sobrinus*, and *S. mutans* [30]. Moreover, plant extracts are the most frequent natural resource for application in medicine. Recently, Mediterranean herbs have been evaluated for their antibacterial and antibiofilm formation activities against *S. mutans*. The biofilm formation of *S. mutans* was significantly inhibited by methanol extracts of *Cistus creticus*, *Cistus monspeliensis*, *Rosmarinus officinalis*, *Salvia sclarea*, and *Thymus longicaulis* at concentrations of 0.60 mg/mL, 0.60 mg/mL, 1.25 mg/mL, 2.50 mg/mL, and 5.00 mg/mL, respectively [31]. In Asia, the root of *Glycyrrhiza uralensis*, a licorice that is an important traditional Chinese herbal medicine, was observed to have antibacterial properties at a concentration of 25 $\mu g/ml$ against *S. mutans* [32]. Some Thai herbal formulas used for dental caries have been reported to suppress the cariogenic properties of *S. mutans* by disrupting its acid formation and quorum sensing abilities. They significantly inhibited the acidogenesis of *S. mutans* without affecting the cell viability and reduced the violacein production of *Chromobacterium violaceum*, indicating the promising anti-quorum sensing activity of the extracts [33]. Therefore, the present study particularly demonstrated the antibacterial and anti-biofilm activities of three herbal plants that were previously widely formulated in many remedies of Thai traditional medicine, including *S. asper* Lour, *C. citratus*, and *S. aromaticum* L., against *S. mutans* and its clinical isolates. The activity of the extracts to inhibit *S. mutans* clinical strains was evaluated in terms of MIC₉₀ and MBC₉₀ values. The results showed that the ethanolic extracts of *S. aromaticum*, *S. asper*, *C. citratus*, and mixed herbs possessed MIC₉₀/MBC₉₀ values of 1.024/2.048, 2.048/4.096, 2.048/8.192, and 0.512/2.048 mg/mL, respectively. Then, molecular docking analysis was performed to model the interaction between a small molecule and a protein at the atomic level, allowing the characterization of the behavior of the plant compounds in the binding site of target GtfB proteins as well as to elucidate fundamental biochemical processes. The principal compounds obtained from the *S. asper* ethanolic extract exhibited lower binding abilities in the range of -7 to -4 kcal/mol. This was higher than the binding score of chlorhexidine standard form 2–4 times. We found

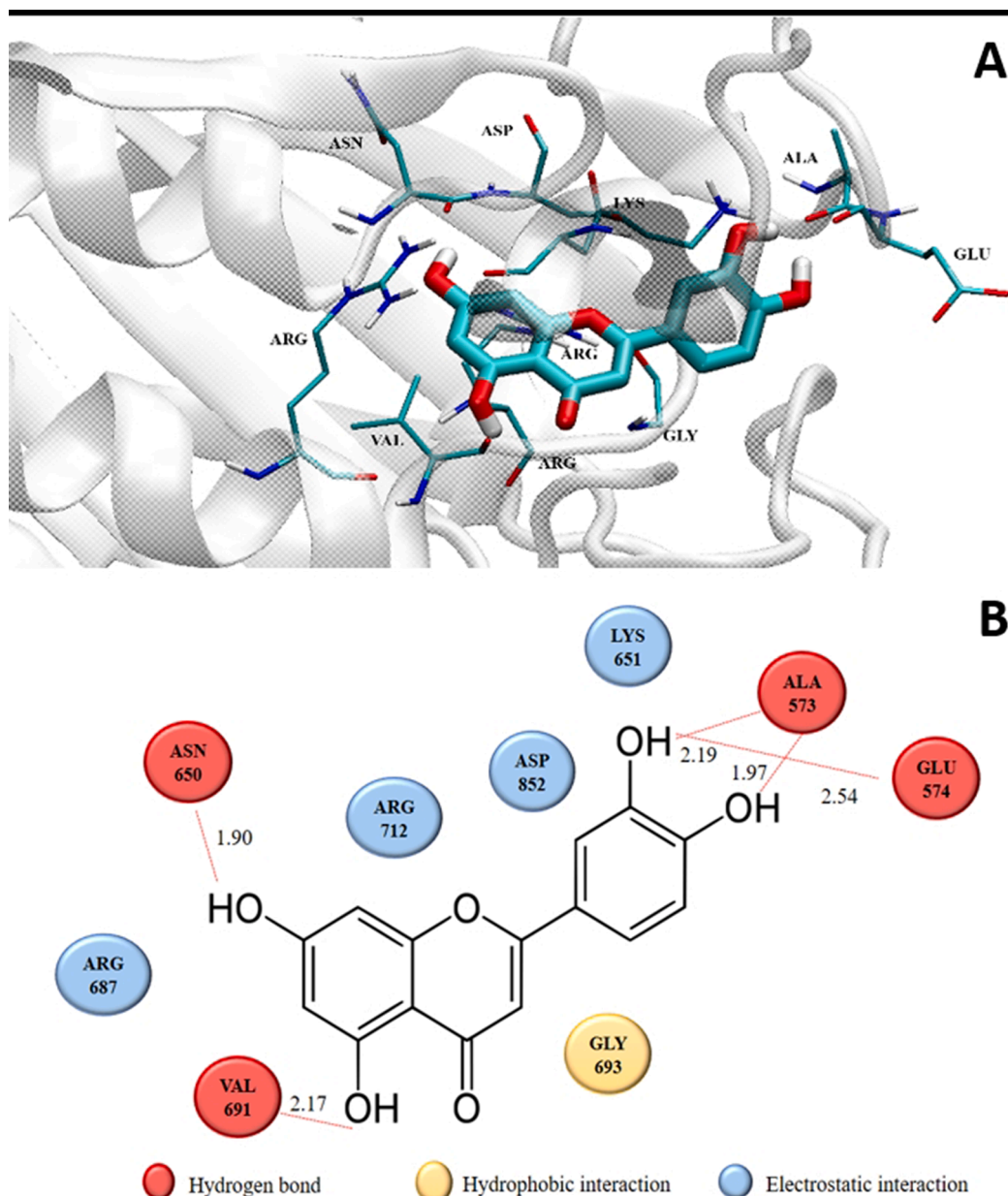


Fig. 3. . (A) Two-dimensional diagram of the proposed residues interacting with luteolin isolated from the *C. citratus* ethanolic extract. (B) 3D structural interaction between luteolin and GtfB amino acids at distances not exceeding 3 Å.

that many compounds isolated from those three herbs demonstrated docking binding scores with the GtfB peptide at less than -9 kcal/mol, including luteolin and kaempferol isolated from *C. Citratus* and quercetin isolated from *S. aromaticum*, suggesting promising activity for the inhibition of *in vitro* bacterial biofilms. However, the biofilm inhibition testing demonstrated that the ethanolic extract of *S. asper*, *S. aromaticum*, *C. citratus*, and mixed herbs at the MIC could reduce *S. mutans* biofilm formation by more than 65% compared with the untreated bacteria. Moreover, modification of bacterial cell surface hydrophobicity was observed in the extract-treated cultures. We speculated that the composition of the plant extract influenced the bacterial cell surface by modifying its hydrophobic characteristics. The hydrophobicity indices of the *S. mutans* isolates were significantly reduced by exposure to a concentration of $1/4 \times \text{MIC}$ of each plant extract and the extract of mixed herbs in this study. The *S. mutans* cell surface exhibited various polymers, such as wall-associated proteins, lipoteichoic acid, serotype-specific protein antigens, and peptidoglycan matrix. Among

these polymers, a cell surface protein antigen (PA) with a molecular mass of 190 kDa is important in surface hydrophobicity [34]. The loss of PA and decreased surface hydrophobicity played a role in mediating bacterial adherence to teeth and oral mucosal surfaces. A decrease in the cell surface hydrophobicity could render microorganisms less readily susceptible to bacterial aggregation and host-cell adhesion [35]. The results of the herbal plant extracts modifying the bacterial cell surface by decreasing hydrophobicity could indicate the effects of the extracts on reducing bacterial virulence factors and the pathogenesis of *S. mutans* infection [36]. Moreover, enhancing the activities of the plant extracts against *S. mutans* was performed by applying nanotechnology. Silver nanoparticles (AgNPs) are synthesized by oxidation and reduction reactions. The antibacterial activities of AgNPs are related to cell wall adherence, penetration of cytoplasmic membranes, and cellular destruction. Previously, silver (Ag) has been employed as an antimicrobial that relies on the release of Ag^+ , which triggers a range of processes resulting in suppressed bacterial growth. The improved release of

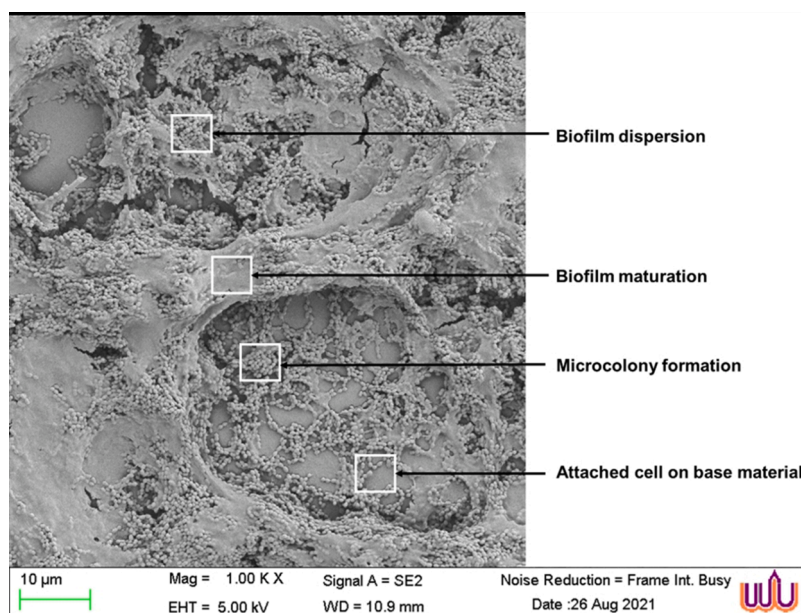


Fig. 4. . SEM images of mature *S. mutans* biofilms at a magnification of $\times 1000$.

silver ions could enhance the bactericidal action [37]. Plant extracts have been employed for the green synthesis of nanomaterials [38]. In addition to the synthetic method, the size and shapes of the AgNPs could affect their antibacterial activity; for example, the antibacterial effect increases with smaller sizes due to the increase in surface area available for ion release and interaction with the bacterial cell. Some evidence has been proposed that the size of AgNPs in the range of 1–10 nm could interact more efficiently with the bacterial cell membrane, [39] and AgNPs with spherical shapes seem to be more effective in bacterial killing than triangles or cylinders [40]. However, AgNPs have shown biocidal effects against a range of bacterial species, both gram-positive and gram-negative, such as *Staphylococcus epidermidis*, *Enterococcus faecalis*, *Vibrio cholerae*, and *Salmonella* spp [39,41]. Although the biocidal action of AgNPs has been attributed mainly to Ag^+ release, the actual mechanism has not yet been completely elucidated. Crucial to their effect is the fact that AgNPs tend to accumulate at the membrane where they progressively aggregate, allowing silver ions to interact with different functional groups, such as sulfate or phosphate, and disturb the function of the bacterial membrane, promoting its rupture and liberating the cytoplasmic content [42]. Recent studies reported that AgNPs prevent the formation of *S. mutans* biofilms on teeth and inhibit quorum sensing to prevent dental caries [24,43]. A green tea extract (*Epigallocatechin gallate*) was used for green synthesized AgNPs to reduce the MIC and MBC against *S. mutans* [44]. In addition, *E. gallate* is able to inhibit *S. mutans* glucosyltransferase, reducing bacterial adherence and biofilm formation. Another interesting application for AgNPs has been their inclusion in formulations for toothpaste with promising antibacterial efficacy against *S. mutans* [45]. This study showed the effects of the green formulated AgNPs on *S. mutans* cells and biofilm structure. SEM images were taken to observe some changes in the topographical features of the bacterial biofilms exposed to the AgNP extracts. The images of *S. mutans* biofilms obtained in this study are similar to the biofilm characteristics from previous reports [46,47], and dense biofilms were observed on the surface of untreated biofilms. Additionally, SEM at 1000x magnification revealed cracks and dark gaps in the biofilm topography, indicating that biofilm fragmentation was more visible in the untreated control biofilms than in the formulated AgNP-treated biofilms. The study proved the effectiveness of AgNP extracts for the prevention and treatment of bacterial biofilm-related oral diseases.

5. Conclusion

The study suggested that the ethanolic extracts of *S. asper*, *S. aromaticum*, and *C. citratus* could be used as natural alternative agents with multiple actions against *S. mutans* infections, as they exhibited antibacterial activities. Modifications of bacterial cells were observed after treatment with the ethanolic extracts by increasing the cell surface hydrophobicity and reducing bacterial biofilm formation within 24 h. The inhibitory actions on bacterial biofilms were confirmed by a demonstration of 3D structural interactions between the compounds isolated from the plant extract and the GtfB amino acids. In particular, the luteolin compound of *C. citratus* showed a high docking score, suggesting that it was an *in vitro* biofilm inhibitor in this study. Moreover, the application of AgNPs formulated from herbal extracts showed potential effects on the modification of bacterial cells, reducing colonization and causing changes in biofilm structure. The findings proved their effectiveness for the prevention and treatment of bacteria-related oral diseases.

Disclosure statement

No conflicts of interest.

Author contributions

All authors read and take responsibility for the integrity of the work as a whole and give their approval for this version to be published.

Funding

This work was supported by Walailak University, Grant Number WU-IRG-64-003, 2021.

CRediT authorship contribution statement

Kulwadee Karnjana: Conceptualization, Methodology, Validation, Formal analysis, Investigation, Writing – original draft, Visualization. **Juntamanee Jewboonchu:** Conceptualization, Methodology, Resources, Software. **Nattisa Niyomtham:** Methodology, Validation, Formal analysis, Investigation, Writing – original draft. **Paveen Tangngamsakul:** Resources, Data curation, Formal analysis. **Kingkan**

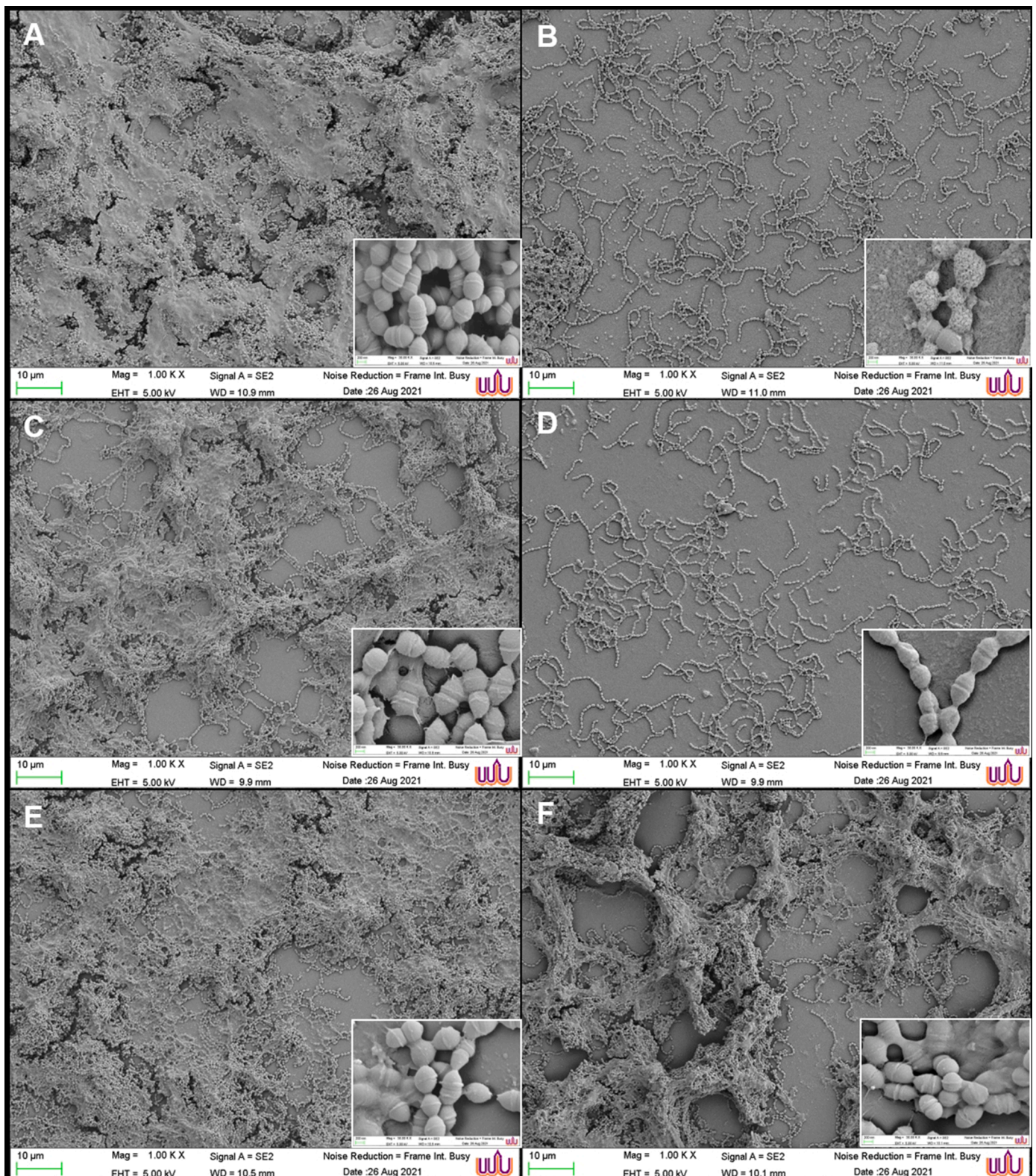


Fig. 5. Comparison of SEM images of the *S. mutans* biofilms treated with the synthesized AgNPs from the herbal ethanolic extracts with untreated biofilms (A). Morphological changes in the bacterial biofilm structure were observed in the treatments of 0.2% chlorhexidine (B), AgNPs from mixed herbs at 1 × MIC (C), AgNPs from *C. citratus* at 1 × MIC (D), AgNPs from *S. aromaticum* at 1 × MIC (E), and AgNPs from *S. asper* at 1 × MIC (F). Each group showed magnifications of × 1000 and × 30,000.

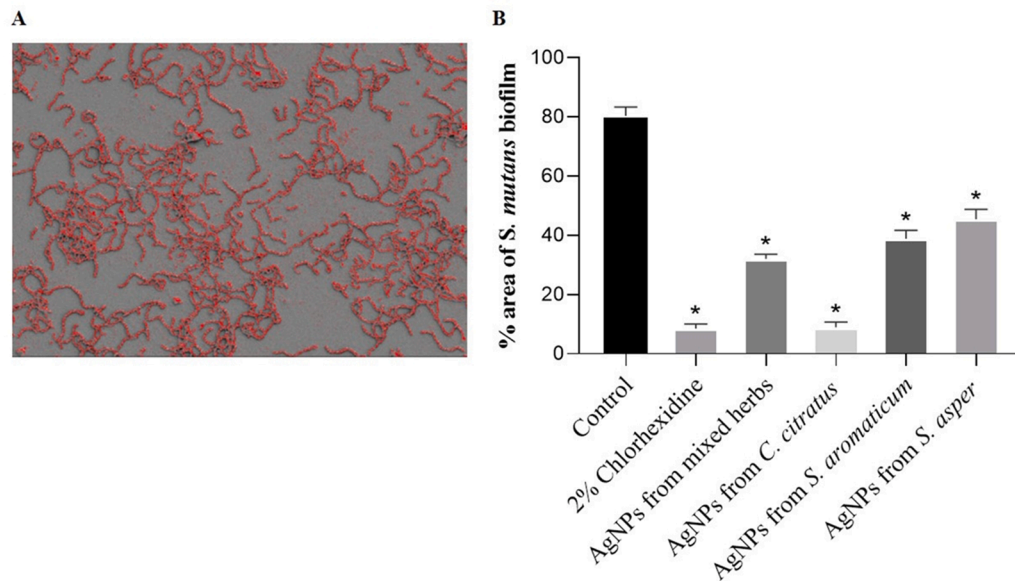


Fig. 6. . The calculation of *S. mutans* reduction of the biofilm surface area using ImageJ software. (A): The pixel of the biofilm area was calculated from the bacterial intensity on the surface. (B): The percentage of biofilm remaining after treatment with the formulated AgNPs from the herbal extracts at concentrations of $1 \times \text{MIC}$ and 0.2% chlorhexidine. The mean value \pm SD from at least duplicates is illustrated. * $p < 0.05$ indicates a significant difference between the treatments and the untreated control.

Bunluepuech: Resources, Writing – original draft. **Lavnaya Goodla:** Writing – review & editing, Software. **Auemphon Mordmuang:** Conceptualization, Methodology, Resources, Writing – review & editing, Supervision, Project administration, Funding acquisition.

Declaration of Competing Interest

Authors have no conflicts of interest to disclose.

Data availability

No data was used for the research described in the article.

Acknowledgments

The authors are grateful to Asst. Prof. Dr. Tanatchaporn Sangfai, School of Pharmacy, Walailak University for cooperation in providing nanoparticle formation methods. We would like to thank the Research Center of Excellence in Innovation of Essential Oil and Bioactive Compounds (WU-COE-66-05), the Research Institute for Health Science, and the Research Center in Tropical Pathobiology, Walailak University, for their kind support and laboratory facilities. Finally, we would like to give special thanks to Mr. Sponge the Frenchie for his special assistance.

References

- [1] A. Muras, A. Otero, Breaking bad: Understanding how Bacterial Communication Regulates Biofilm-Related Oral Diseases, Trends in Quorum Sensing and Quorum Quenching, 2020, pp. 175–185.
- [2] L. Al-Nasser, I.B. Lamster, Prevention and management of periodontal diseases and dental caries in the older adults, Periodontol 84 (1) (2000) 69–83, 2020.
- [3] J.R. John, et al., Prevalence of dental caries, oral hygiene knowledge, status, and practices among visually impaired individuals in Chennai, Tamil Nadu, Int. J. Dent. (2017), 9419648, 2017.
- [4] C.B. André, et al., Modulation of Streptococcus mutans virulence by dental adhesives containing anti-caries agents, Dent. Mater. 33 (10) (2017) 1084–1092.
- [5] K. Rainey, et al., Glycosyltransferase-mediated biofilm matrix dynamics and virulence of streptococcus mutans, Appl. Environ. Microbiol. 85 (5) (2019).
- [6] J.A. Banas, D.R. Drake, Are the mutans streptococci still considered relevant to understanding the microbial etiology of dental caries? BMC Oral Health 18 (1) (2018) 129.
- [7] Y. Lin, et al., Inhibition of Streptococcus mutans biofilm formation by strategies targeting the metabolism of exopolysaccharides, Crit. Rev. Microbiol. 47 (5) (2021) 667–677.
- [8] M.C. Castillo Pedraza, et al., Extracellular DNA and lipoteichoic acids interact with exopolysaccharides in the extracellular matrix of Streptococcus mutans biofilms, Biofouling 33 (9) (2017) 722–740.
- [9] Y. Jiao, et al., Advancing antimicrobial strategies for managing oral biofilm infections, Int. J. Oral Sci. 11 (3) (2019) 28.
- [10] A. Rauf, N. Jehan, Natural products as a potential enzyme inhibitors from medicinal plants, Enzyme Inhibitors and Activators 165 (2017) 177.
- [11] R.S. Kumar, et al., Evaluation of antihyperglycemic and antioxidant properties of Streblus asper Lour against streptozotocin-induced diabetes in rats, Asian Pac. J. Trop. Dis. 2 (2) (2012) 139–143.
- [12] S. Rastogi, D.K. Kulshreshtha, A.K. Rawat, Shakhotaka): a review of its chemical, pharmacological and ethnomedicinal properties, Evid. Based Complement Alternat. Med. 3 (2) (2006) 217–222.
- [13] G.D. Mogoşanu, et al., 11 - natural products used for food preservation, Food Preserv. (2017) 365–411.
- [14] G. Shah, et al., Scientific basis for the therapeutic use of Cymbopogon citratus, stapf (Lemon grass), J. Adv. Pharm. Technol. Res. 2 (1) (2011) 3–8.
- [15] V. Biscola, et al., Isolation and characterization of a nisin-like bacteriocin produced by a Lactococcus lactis strain isolated from charqui, a Brazilian fermented, salted and dried meat product, Meat. Sci. 93 (3) (2013) 607–613.
- [16] S.F. Melo, et al., Effect of the Cymbopogon citratus, Maytenus ilicifolia and Baccharis genistelloides extracts against the stannous chloride oxidative damage in Escherichia coli, Mutat. Res. 496 (1–2) (2001) 33–38.
- [17] G.E. Batiha, et al., Syzygium aromaticum L. (Myrtaceae): traditional uses, bioactive chemical constituents, pharmacological and toxicological activities, Biomolecules 10 (2) (2020).
- [18] F.S. Al-Khattaf, Gold and silver nanoparticles: green synthesis, microbes, mechanism, factors, plant disease management and environmental risks, Saudi J. Biol. Sci. 28 (6) (2021) 3624–3631.
- [19] A. Guleria, et al., Room temperature ionic liquid assisted rapid synthesis of amorphous Se nanoparticles: their prolonged stabilization and antioxidant studies, Mater. Chem. Phys. 253 (2020), 123369.
- [20] H. Koo, et al., Exopolysaccharides produced by Streptococcus mutans glucosyltransferases modulate the establishment of microcolonies within multispecies biofilms, J. Bacteriol. 192 (12) (2010) 3024–3032.
- [21] A. Mordmuang, et al., Effects of rhodomyrtus tomentosa leaf extract on staphylococcal adhesion and invasion in bovine udder epidermal tissue model, Nutrients 7 (10) (2015) 8503–8517.
- [22] A. Mordmuang, S.P. Voravuthikunchai, Rhodomyrtus tomentosa (Aiton) Hassk. leaf extract: an alternative approach for the treatment of staphylococcal bovine mastitis, Res. Vet. Sci. 102 (2015) 242–246.
- [23] J. Jewboonchu, et al., Atomistic insight and modeled elucidation of connesine towards Pseudomonas aeruginosa efflux pump, J. Biomol. Struct. Dyn. 40 (4) (2022) 1480–1489.
- [24] M.K. Rai, et al., Silver nanoparticles: the powerful nanoweapon against multidrug-resistant bacteria, J. Appl. Microbiol. 112 (5) (2012) 841–852.
- [25] J.A. Lemos, et al., The biology of streptococcus mutans, Microbiol. Spectr. 7 (1) (2019).
- [26] C. Janakiram, et al., Effectiveness of herbal oral care products in reducing dental plaque & gingivitis - a systematic review and meta-analysis, BMC Complement. Med. Ther. 20 (1) (2020) 43.
- [27] H. Koo, M.L. Falsetta, M.I. Klein, The exopolysaccharide matrix: a virulence determinant of cariogenic biofilm, J. Dent. Res. 92 (12) (2013) 1065–1073.

- [28] A. Amer, et al., Antagonistic activity of bacteria isolated from the Periplaneta Americana L. Gut against some multidrug-resistant human pathogens, *Antibiotics* 10 (3) (2021) 294.
- [29] M. Chowdaiah, P. Sharma, P. Dhamodhar, A study on phytochemicals from medicinal plants against multidrug resistant streptococcus mutans, *Int. J. Pept. Res. Ther.* 25 (4) (2019) 1581–1593.
- [30] Z. Tong, et al., Nisin inhibits dental caries-associated microorganism *in vitro*, *Peptides* 31 (11) (2010) 2003–2008.
- [31] J. Hickl, et al., Mediterranean herb extracts inhibit microbial growth of representative oral microorganisms and biofilm formation of Streptococcus mutans, *PLoS ONE* 13 (12) (2018), e0207574.
- [32] Y. Chen, et al., Lollipop containing Glycyrrhiza uralensis extract reduces Streptococcus mutans colonization and maintains oral microbial diversity in Chinese preschool children, *PLoS ONE* 14 (8) (2019), e0221756.
- [33] S. Sanpinit, et al., Selected Thai traditional polyherbal medicines suppress the cariogenic properties of Streptococcus mutans by disrupting its acid formation and quorum sensing abilities, *S. Afr. J. Bot.* 144 (2022) 355–363.
- [34] T. Koga, et al., Surface hydrophobicity, adherence, and aggregation of cell surface protein antigen mutants of Streptococcus mutans serotype c, *Infect. Immun.* 58 (2) (1990) 289–296.
- [35] H. Ohta, et al., Characterization of a cell-surface protein antigen of hydrophilic Streptococcus mutans strain GS-5, *J. Gen. Microbiol.* 135 (4) (1989) 981–988.
- [36] M. Matsumoto-Nakano, et al., Contribution of cell surface protein antigen c of Streptococcus mutans to platelet aggregation, *Oral Microbiol. Immunol.* 24 (5) (2009) 427–430.
- [37] T.C. Dakal, et al., Mechanistic basis of antimicrobial actions of silver nanoparticles, *Front. Microbiol.* 7 (2016) 1831.
- [38] A. Kharabi Masooleh, A. Ahmadikeh, A. Saidi, Green synthesis of stable silver nanoparticles by the main reduction component of green tea (Camellia sinensis L.), *IET Nanobiotechnol.* 13 (2) (2019) 183–188.
- [39] S.M. Zayed, et al., Biofilm Formation By Streptococcus Mutans and Its Inhibition By Green Tea Extracts, 11, *AMB Express*, 2021, p. 73.
- [40] M.A. Raza, et al., Size- and shape-dependent antibacterial studies of silver nanoparticles synthesized by wet chemical routes, *Nanomaterials (Basel)* 6 (4) (2016).
- [41] E. Sánchez-López, et al., Metal-based nanoparticles as antimicrobial agents: an overview, *Nanomaterials* 10 (2) (2020).
- [42] S.H. Lee, B.H. Jun, Silver nanoparticles: synthesis and application for nanomedicine, *Int. J. Mol. Sci.* 20 (4) (2019).
- [43] I.X. Yin, et al., Use of silver nanomaterials for caries prevention: a concise review, *Int. J. Nanomed.* 15 (2020) 3181–3191.
- [44] I.X. Yin, et al., Developing biocompatible silver nanoparticles using epigallocatechin gallate for dental use, *Arch. Oral Biol.* 102 (2019) 106–112.
- [45] F. Ahmed, et al., Antimicrobial efficacy of nanosilver and chitosan against Streptococcus mutans, as an ingredient of toothpaste formulation: an *in vitro* study, *J. Indian Soc. Pedod. Prev. Dent* 37 (1) (2019) 46–54.
- [46] Y. Asahi, et al., Simple Observation of Streptococcus mutans Biofilm By Scanning Electron Microscopy Using Ionic Liquids, 5, *AMB Express*, 2015, p. 6.
- [47] T. Ouidir, B. Gabriel, Y. Nait Chabane, Overview of multi-species biofilms in different ecosystems: wastewater treatment, soil and oral cavity, *J. Biotechnol.* 350 (2022) 67–74.